Level structure of ^{31}S: From low excitation energies to the region of interest for hydrogen burning in novae through the ^{30}P(p,γ)^{31}S reaction

D. T. Doherty,[1,*] P. J. Woods,[1] G. Lotay,[1,†] D. Seweryniak,[2] M. P. Carpenter,[2] C. J. Chiara,[3,2] H. M. David,[1,‡]
R. V. F. Janssens,[2] L. Trache,[4,§] and S. Zhu[2]

[1]*School of Physics and Astronomy, University of Edinburgh, Edinburgh EH9 3JZ, United Kingdom*
[2]*Physics Division, Argonne National Laboratory, Argonne, Illinois 60439, USA*
[3]*Department of Chemistry and Biochemistry, University of Maryland, College Park, Maryland 20742, USA*
[4]*Cyclotron Institute, Texas A&M University, College Station, Texas 77843, USA*
(Received 7 January 2014; revised manuscript received 14 March 2014; published 23 April 2014)

Comprehensive measurements of the excitation energy and spin-parity assignments for states in ^{31}S are presented, from the first excited state, up to energies relevant for the ^{30}P(p,γ)^{31}S reaction in ONe novae. This reaction rate strongly influences heavy element abundances in novae ejecta. States in ^{31}S are paired with their ^{31}P analogues using γ rays detected with the Gammasphere detector array following the ^{28}Si(^{4}He, n) fusion-evaporation reaction. The evolution of mirror energy differences is explored and the results are compared with new shell-model calculations. The excellent agreement observed in this work between experimental data and shell-model calculations provides confidence in using computed estimates in situations where experimental data are unavailable.

I. INTRODUCTION

For nuclei in the sd-shell lying close to the valley of stability it is possible to explore the almost complete level structure from the ground state to the region above the particle emission threshold. Such data represent a detailed challenge for the shell-model and can be used to explore mirror energy differences (MEDs) in detail as a function of excitation energy and angular momentum. A recent such example was reported for the $T = 1/2$, $A = 27$ system [1]. States above the proton threshold can play a critical role in explosive hydrogen burning scenarios. A precise knowledge of the excitation energy and spin-parity of these states is required for reliable reaction rate estimates in the absence of direct measurements. A detailed knowledge of the states, including below the proton threshold, is important to establish the reliability of these assignments and consistency with theory. In the present paper, we report on a comprehensive γ-spectroscopy study of levels in ^{31}S from the first excited state to the region close to the proton threshold (at 6130.9(4) keV [2]) of relevance for the ^{30}P(p,γ)^{31}S reaction which strongly influences the production of heavy elements in oxygen-neon ONe novae [3,4]. A direct measurement of this reaction using ISOL radioactive beams at the energy appropriate for hydrogen burning in novae is not presently feasible. Our results for states lying above the proton threshold in ^{31}S have previously been reported in Ref. [5]. In Ref. [5] new, low-spin resonances were identified above the proton threshold in ^{31}S which were not observed in the previous

heavy-ion fusion-evaporation reaction performed by Jenkins *et al.* [6,7]. The identification of these low-spin resonances leads to a large increase in the predicted ^{30}P(p,γ)^{31}S reaction rate for nova temperatures implying a larger flux of material processed towards high-Z elements in nova environments. The assignment of these low-spin resonances is now reinforced in the present work by investigating the complete level structure of ^{31}S, from the ground state up to the energies of interest for hydrogen burning in novae.

II. EXPERIMENTAL DETAILS

A $\sim$10 pnA, 22-MeV beam of ^{4}He^{1+} ions from the ATLAS accelerator at Argonne National Laboratory was used to bombard a 120 μg/cm^2-thick ^{28}Si target for a period of 71 h. At this beam energy, the compound nucleus, ^{32}S, decays via the single-neutron, -proton and -α particle-evaporation channels leading to residues of ^{31}S, ^{31}P, and ^{28}Si, respectively. Prompt γ rays were detected with the Gammasphere detector array of Compton-suppressed Ge detectors [8]. In this instance, it was operated with the trigger requirement of two coincident γ rays. The data were then sorted offline into standard γ-γ matrices and γ-γ-γ cubes from which level schemes could be constructed using the RADWARE software package [9]. Energy and efficiency calibrations were performed using standard ^{152}Eu and ^{56}Co sources. An additional 6.129-MeV line in ^{16}O, from the ^{13}C(α,n)^{16}O reaction, was also used as a calibration point to improve the energy calibration for high-energy γ rays. The source data and ^{16}O transition were then also used to apply a correction for the known nonlinearity of the Gammasphere detector array, this step is crucial in obtaining accurate γ-ray energies, particularly for high energy γ rays.

A full angular distribution analysis was performed for strong transitions. γ intensities were extracted and then corrected for the detection efficiency of each Gammasphere ring before being fitted as a function of detection angle, with respect

*d.t.doherty@sms.ed.ac.uk

†Present address: Department of Physics, University of Surrey, Guildford, GU2 7XH, United Kingdom.

‡Present Address: Physics Division, Argonne National Laboratory, Argonne, Illinois 60439, USA.
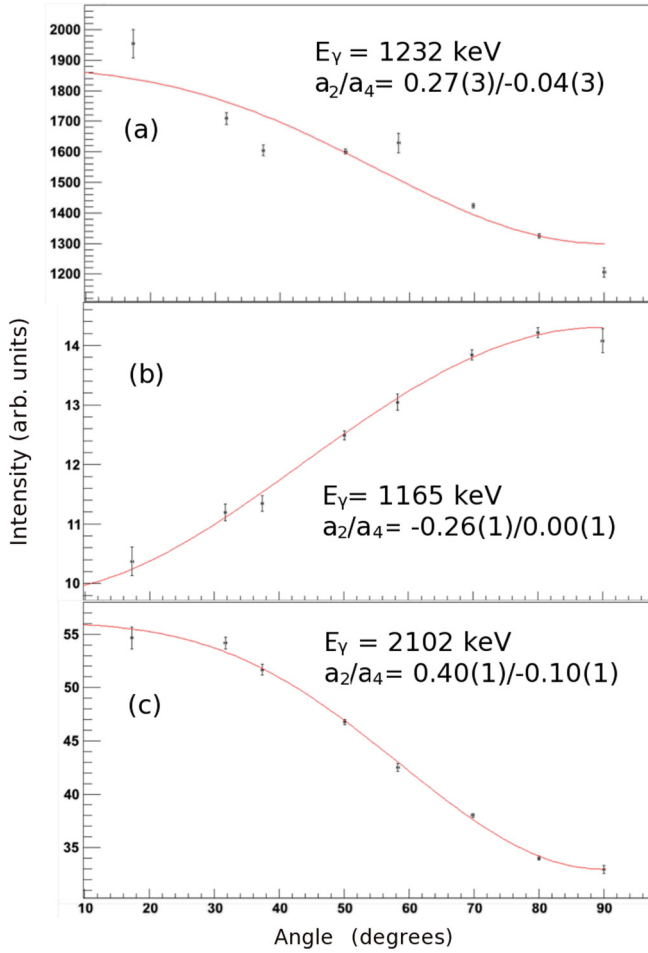
§Present address: IFIN-HH, Bucharest-Magurele, Romania.

FIG. 1. (Color online) Typical γ-ray angular distributions obtained in the present work. (a) An example of a $\Delta J = 0$ transition between two $7/2^+$ states. (b) Example of a $\Delta J = 1$ transition between $7/2^-$ and $5/2^+$ states. (c) Example of a $\Delta J = 2$ transition between $7/2^+$ and $3/2^+$ states. Corrections for the detection efficiency of various rings of Gammasphere were taken into account.

to the beam axis, using the function $W(\theta) = a_0\{1 + a_2 P_2(\cos\theta) + a_4 P_4(\cos\theta)\}$. Where the Legendre polynomials

$P_2(\cos\theta) = \frac{1}{2}(3\cos^2\theta - 1)$ and $P_4(\cos\theta) = \frac{1}{8}(35\cos^4\theta - 30\cos^2\theta + 3)$. The free parameters a_2 and a_4 were then used to deduce the character of the observed γ transition. Examples of typical angular distribution obtained in the present work for $\Delta J = 0$, ± 1, and ± 2 are presented in Fig. 1. The a_2 and a_4 values depend on the initial and final spins of the states involved, however, by fitting known transitions observed in both ^{31}S and ^{31}P trends could be established. Positive values for a_2 with $a_4 \sim 0$ signify $\Delta J = 0$ transitions, a negative a_2 with $a_4 \sim 0$, $\Delta J = 1$, and a positive value for a_2 and a negative a_4 indicating a $\Delta J = 2$ transition. Caution must, therefore, be taken when considering pure nonstretched ($\Delta J = 0$) dipole and quadrupole ($\Delta J = 2$) transitions as the a_2 and a_4 values may be similar. However, in these cases spin-parity assignments may still be made by considering extra information such as the observed decay branches or by appealing to the known level structure of the mirror partner. This approach, where a full angular distribution analysis for strong γ rays is performed, has been utilized successfully in the past to assist with making spin-parity assignments, for example Refs. [1,10].

III. RESULTS

In an earlier publication [5] based on this data set, Doherty *et al.* presented new data on key, proton-unbound states in ^{31}S relevant for calculating the ^{30}P$(p,\gamma)^{31}$S reaction rate in ONe novae. Here, we expand on that work by presenting new information on all states in ^{31}S up to an excitation energy of 6.7 MeV, the largest energy of interest in ONe nova environments.

Table I presents recoil corrected excitation energies (E_x), γ-ray energies as measured in the laboratory (E_γ), γ-ray intensities, angular distribution coefficients (a_2 and a_4), and spin-parity assignments for states in ^{31}S for the current work, together with the excitation energy of the analog states in ^{31}P. Coincidence spectra derived from analysis of the γ-γ matrix and the γ-γ-γ cube are shown in Figs. 2, 3, and 4, respectively. Peak centroids were then determined from these spectra by fitting Gaussian peaks on a flat background. Excitation energies were then determined by summing the γ-ray energies after applying a recoil correction. For a small number of cases multiple cascades are observed from the same level which do not yield the same excitation energy, for example the 6138-keV

TABLE I. γ-ray laboratory energies, intensities, angular distribution coefficients, spin-parity assignments, and proposed mirror assignments from the present work. It should be noted that only the statistical uncertainties for the intensities are quoted. In the first column the ^{31}S excitation energies are corrected for the recoil of the compound nucleus.

E_x (keV) (Present work)	E_γ (keV) (Present work)	I_γ(%)	a_2/a_4	ΔJ	Assignment	^{31}P mirror energy assignment
1248.5(1)	1248.5(1)	$\equiv$100.0	$-0.16(1)/-0.03(2)$	1	$3/2^+\rightarrow1/2^+$	1266
2234.5(2)	986.0(2)[a]	1.0(2)			$5/2^+\rightarrow3/2^+$	2234
	2234.4(2)	18.1(4)	$0.20(2)/-0.28(2)$	2	$5/2^+\rightarrow1/2^+$	
3076.1(10)	1827.5(10)[a]	0.4(1)	$0.09(3)/-0.04(4)$	1	$1/2^+\rightarrow3/2^+$	3134
3284.7(2)	1049.8(2)	6.7(2)			$5/2^+\rightarrow5/2^+$	3295
	2035.5(2)	35.8(7)	$-0.70(3)/0.00(2)$	1	$5/2^+\rightarrow3/2^+$	
	3284.4(2)	6.5(2)	$0.15(2)/-0.17(2)$	2	$5/2^+\rightarrow1/2^+$	
3351.3(2)	2101.7(2)	49.8(3)	$0.40(1)/-0.10(1)$	2	$7/2^+\rightarrow3/2^+$	3415
3433.3(5)	2184.7(5)[a]	0.4(1)			$3/2^+\rightarrow3/2^+$	3506
4086.1(16)	2837.5(16)[a]	2.8(2)	$-0.12(2)/-0.06(3)$	1	$5/2^+\rightarrow3/2^+$	4191

TABLE I. (*Continued.*)

E_x (keV) (Present work)	E_γ (keV) (Present work)	$I_\gamma(\%)$	a_2/a_4	ΔJ	Assignment	^{31}P mirror energy assignment
4208.3(5)	2959.6(5)[a]	0.7(1)	0.12(3)/−0.04(3)	1	$3/2^+ \rightarrow 3/2^+$	4260
4449.6(3)	1164.9(2)	28.3(5)	−0.26(1)/0.00(1)	1	$7/2^- \rightarrow 5/2^+$	4431
4527.8(2)	3279.1(2)[a]	0.4(1)			$3/2^+ \rightarrow 3/2^+$	4593
4583.4(3)	1232.1(2)	3.5(2)	0.27(3)/−0.04(3)	0	$7/2^+ \rightarrow 7/2^+$	4634
	1298.7(1)	2.8(2)	−0.77(2)/−0.05(2)	1	$7/2^+ \rightarrow 5/2^+$	
	3334.2(8)[a]	2.4(2)	0.27(4)/−0.27(4)	2	$7/2^+ \rightarrow 3/2^+$	
4602(18)[b]	*unobserved*					
4710.1(8)	1425.3(8)	0.3(1)			$5/2^+ \rightarrow 5/2^+$	4783
4867.5(3)	3619.0(3)[a]	3.0(2)	−0.04(2)/−0.07(2)	1	$1/2^+ \rightarrow 3/2^+$	5015
4971.2(20)	3722.5(20)[a]	0.9(2)	0.08(7)/0.05(11)	0,1	$(1/2,3/2)^- \rightarrow 3/2^+$	5015
5023.9(3)	1672.6(2)[a]	1.0(2)	−0.27(4)/−0.04(4)	1	$5/2^+ \rightarrow 7/2^+$	5116
	3774.0(30)[a]	0.7(1)			$5/2^+ \rightarrow 3/2^+$	
5157.5(20)	(3909.9(20))[a]	0.3(1)			$1/2^+ \rightarrow 3/2^+$	5257
5301.7(3)	1950.3(2)	14.5(2)	−0.28(1)/−0.02(1)	1	$9/2^+ \rightarrow 7/2^+$	5343
5401.5(8)	2050.2(8)[a]	1.9(2)	−0.42(6)/−0.07(8)	1	$5/2^+ \rightarrow 7/2^+$	5530
5439.1(29)[c]	*unobserved*					5559
5518.3(3)	2166.7(10)[a]	0.5(1)			$5/2^+ \rightarrow 7/2^+$	5672
	4269.5(3)[a]	1.8(4)	−0.38(2)/−0.06(3)	1	$5/2^+ \rightarrow 3/2^+$	
5675.8(6)	2325.2(6)[a]	1.3(2)	0.21(6)/−0.09(6)	0	$7/2^+ \rightarrow 7/2^+$	5774
5775.1(15)[c]	*unobserved*				$5/2^+$	5988
5824.2(29)[c]	*unobserved*				$9/2^+$	5892
5891.5(20)	4642.6(20)[a]	0.7(1)	0.16(11)/0.07(9)	0	$3/2^+ \rightarrow 3/2^+$	6158
5977.2(7)	1393.8(6)	0.8(2)			$(9/2^+) \rightarrow 7/2^+$	6078
6138.3(21)	2785.7(20)[a]	0.5(1)			$(3/2,7/2)^+ \rightarrow 7/2^+$	6233
	4889.5(6)[a]	0.5(1)	0.15(12)/0.03(14)	0,2	$(3/2,7/2)^+ \rightarrow 3/2^+$	
6158.5(5)	1707.6(3)	1.7(2)	0.22(2)/−0.07(3)	0	$7/2^+ \rightarrow 7/2^-$	6399
	2873.9(6)	0.5(1)			$7/2^+ \rightarrow 5/2^+$	
6255.3(5)[d]	*unobserved*				$1/2^+$	6337
6280.6(2)[d]	*unobserved*				$3/2^+; T = 3/2$	6381
6327.0(5)	5077.7(5)[a]	0.5(1)	0.14(7)/0.10(9)	0	$3/2^- \rightarrow 3/2^+$	6496
6357.3(2)	5108.0(2)[a]	0.7(1)	−0.25(5)/−0.01(7)	1	$5/2^- \rightarrow 3/2^+$	6594
6376.9(4)	1925.7(2)	9.6(2)	−0.39(1)/−0.02(1)	1	$9/2^- \rightarrow 7/2^-$	6502
	3025.4(3)[a]	5.2(2)	−0.46(1)/−0.01(2)	1	$9/2^- \rightarrow 7/2^+$	
6392.5(2)	5143.1(2)[a]	1.5(1)	−0.25(3)/−0.09(3)	1	$5/2^+ \rightarrow 3/2^+$	6461
6394.2(2)	1091.2(4)	3.1(2)	−0.37(5)/−0.01(1)	1	$11/2^+ \rightarrow 9/2^+$	6453
	3042.9(1)	11.0(2)	0.26(1)/−0.26(1)	2	$11/2^+ \rightarrow 7/2^+$	
6402(2)[e]	*unobserved*					
6541.9(4)	5292.5(4)[a]	0.6(1)	0.13(4)/−0.03(6)	0	$3/2^- \rightarrow 3/2^+$	6610
6583.1(20)	3298.0(20)[a]	0.3(1)			$(5/2,7/2)^- \rightarrow 5/2^+$	6842
6636.1(7)	2184.9(4)	1.6(2)			$9/2^- \rightarrow 7/2^-$	6796
	3284.7(2)	6.9(2)	−0.48(1)/−0.02(2)	1	$9/2^- \rightarrow 7/2^+$	

[a]Gamma rays not reported in the heavy-ion fusion reaction of Jenkins *et al.* [6,7].
[b]Not observed in the present study. Level listed in 2013 Nuclear Data Evaluation [11] from reported tentative population in (^{3}He, α) [12], but likely does not exist.
[c]Levels not observed in the present study. Excitation energies and spin-parity assignments from Wrede *et al.* [13,14].
[d]Levels not observed in the present study. Excitation energies and spin-parity assignments taken from the 2013 Nuclear Data Evaluation [11].
[e]Level not observed in the present study. The excitation energy and suggested spin-parity assignment is from Irvine *et al.* [15].

state, for these cases the uncertainty on the derived excitation energy is inflated. A detailed comparison is then made with the well-studied mirror nucleus, ^{31}P, and also with new shell-model calculations.

The data obtained in the present work provide a further demonstration of the power of isospin symmetry in *sd*-shell nuclei. The γ-decay schemes for states in ^{31}P and ^{31}S at low-excitation energies are presented in Figs. 5(a) and 5(b). Excellent agreement is clearly observed in the γ-decay modes

and branching ratios for analog, excited states in the $A = 31$ mirror system. Departures from strict isospin symmetry are, however, interesting. Here, as observed in Ref. [6], the $7/2_1^-$, 4450-keV excited state in ^{31}S is observed to decay with a single decay branch to the $5/2_2^+$ level. For the $7/2_1^-$, 4431-keV analog state in ^{31}P, however, an additional strong γ-decay branch is observed to the $5/2_1^+$ level. Furthermore, notable differences in the intensities of mirror γ-decay transitions are observed. For example in the decay of the $5/2_1^+$ states. Such observations
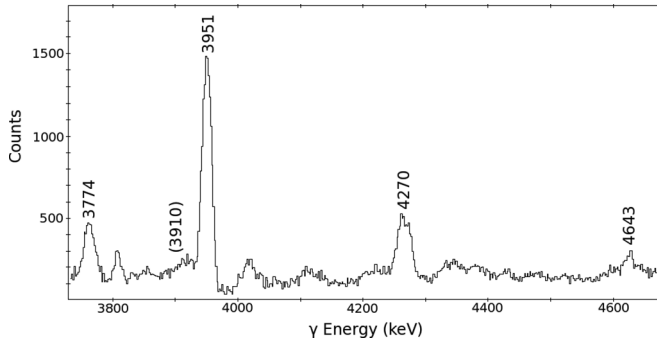
FIG. 2. γ-ray spectrum gated on the 1249-keV transition in ^{31}S. Energies of transitions observed in ^{31}S are labeled in keV. The tentative 3910-keV transition is placed in parenthesis. The 3951-keV transition is from a higher-lying ^{31}S level reported in the high-spin study performed by Jenkins *et al.* [6,7].

are consistent with differences observed between γ-decay modes of mirror states reported in other sd-shell nuclei, e.g., Refs. [1,16]. Also shown, in Fig. 6 is the full ^{31}S decay scheme observed in the present work.

It can be seen from Fig. 8 that all states in ^{31}S up to an excitation energy of 6.7 MeV have been identified and matched to their ^{31}P mirror analog states. Furthermore, good agreement between even-parity states in ^{31}S and shell-model calculations was found as demonstrated in Fig. 7. States of particular interest or ones requiring additional explanation are discussed in the text below.

The previous γ-ray spectroscopy of the $A = 31$ mirror system by Jenkins *et al.* [6,7] focused on high-spin states only but, nevertheless, proved to be a useful starting point for this study, where the full level structure of the nucleus ^{31}S is investigated. The first state not discussed by Jenkins *et al.* is the 3076-keV, $1/2^+$ level. Examination of the decay branches reported for its analogue level in ^{31}P reveal that the dominant decay branch for this state is expected to be direct to the ground state. The trigger condition used in the present work, however, prevents the observation of such a decay branch as the state is fed only weakly from higher-lying levels. Here, we do, however, observe a transition to the $3/2_1^+$ level; with the observed, isotropic angular distribution being consistent with a decay from a $J = 1/2$ state (see Table I). The 3351-keV state
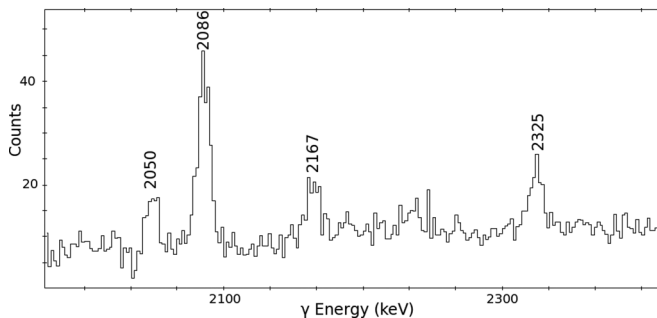

FIG. 3. γ-ray spectrum gated on both the 1249- and 2102-keV transitions in ^{31}S. Energies of observed transitions are given in keV. The 2086-keV transition is from a higher-lying ^{31}S level reported in the high-spin study performed by Jenkins *et al.* [6,7].

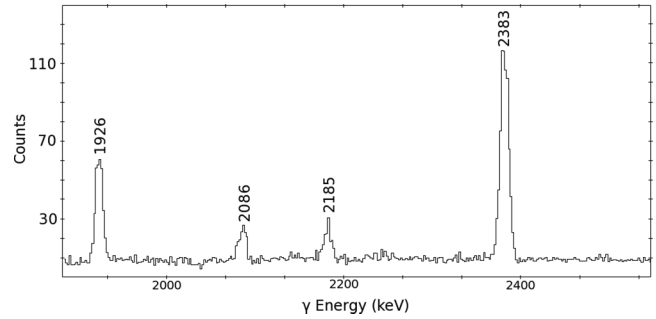FIG. 4. γ-ray spectrum gated on both the 1165- and 2036-keV transitions in ^{31}S. Energies of observed transitions are given in keV. The 2086- and 2383-keV transitions are from higher-lying ^{31}S levels reported in the high-spin study performed by Jenkins *et al.* [6,7].

was also reported in the work of Jenkins *et al.* [6,7] who pair it with the 3415-keV mirror level in ^{31}P and, hence, assign a spin-parity $7/2^+$. However, we note that in the latest Nuclear Data Evaluation [11] the spin-parity of the 3351-keV level is listed as uncertain. In this work we observe a clear $\Delta J = 2$ transition from this state to the $3/2_1^+$ level, as shown in Fig. 1(c) confirming the $7/2^+$ assignment. Knowledge of the spin-parity of this state is particularly important as transitions are observed to feed it from proton-unbound levels which play a role in the key ^{30}P$(p,\gamma)^{31}$S capture reaction in ONe novae outbursts.

Additional low-spin states are observed at excitation energies of 3433, 4086, and 4208 keV which were not reported by Jenkins *et al.* [6,7]. All are observed to have decay branches toward the $3/2_1^+$ level. In addition all are expected to have large decay branches toward the ground state, which are not observable in this work.

For excitation energies greater than 4.4 MeV, the minimum energy to promote a particle from the sd to f shell [6], odd-parity states are observed. The first odd-parity state at 4450 keV was reported by Jenkins *et al.* [6]. However, the spin-parity is listed as uncertain in the latest Nuclear Data Evaluation [11]. Here, we observe its decay via the 1165-keV γ ray to the $5/2_2^+$ level, with an angular distribution characteristic of a $\Delta J = 1$ transition, see Fig. 1(b). As there are no candidate $3/2$ or $7/2^+$ levels that exhibit this decay branch in the mirror nucleus, or are predicted by shell-model calculations, we conclude that this is the $7/2_1^-$ level, the analog of the 4431-keV state in ^{31}P. As was the case with the 3351-keV level, transitions are observed to this state from key, proton-unbound levels. Hence, precise knowledge of its spin-parity is critical. Another bound, odd-parity state is observed at 4971 keV via its γ decay to the $3/2_1^+$ level. Angular distribution coefficients of $a_2 = 0.08(7)$ and $a_4 = 0.05(11)$ do not permit a definitive spin-parity assignment as they are consistent with both a $\Delta J = 0$ and an isotropic distribution at the $\sim 1\sigma$ level. Therefore, we adopt the previous spin-parity assignment of $(1/2,3/2)^-$ [11].

A neighboring odd-parity state at 4867.5 keV is listed in the Nuclear Data Evaluation [11] with a spin-parity of $(1/2,3/2)^-$. In the present work, a state is observed in ^{31}S with an excitation energy of 4867.5(3) keV. Angular distribution analysis of its γ decay to the $3/2_1^+$ level yielded a_2 and a_4 coefficients of
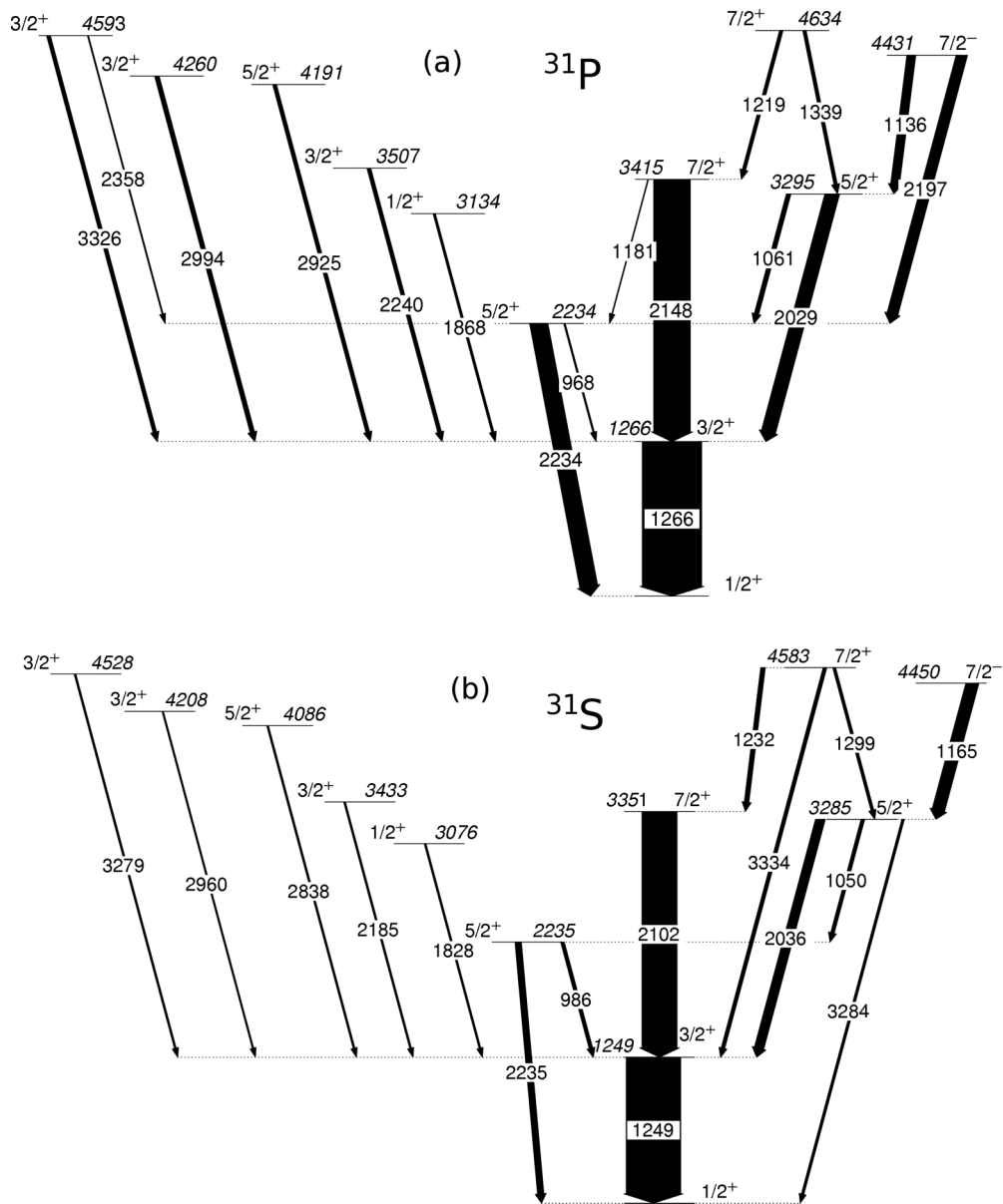
FIG. 5. Comparison of the decay branches observed in the present work for the $A = 31$ mirror pair (a) ^{31}P and (b) ^{31}S for states with low excitation energy. The γ-ray energies are given in keV, while the widths of the arrows represent the observed intensity of the transitions.

$-0.04(2)$ and $-0.07(2)$, respectively. These coefficients are consistent with an isotropic distribution implying either a $1/2^+$ or $1/2^-$ assignment for the 4868-keV state. However, we note that a $1/2^-$ state is not observed in this energy range, in the well studied mirror-nucleus ^{31}P. Furthermore, shell-model calculations predict an additional $1/2^+$ state in this energy region. This level is also observed to be populated in the β decay of ^{31}Cl [17], where the population of negative opposite-parity states is suppressed with respect to even-parity states. Therefore, we assign to the 4868-keV level a spin-parity of $1/2^+$.

Also of interest in this energy region is an unobserved state with an excitation energy of 4602(18) keV, see Table I. Although listed in the recent Nuclear Data evaluation [11], this level has only been observed in a single ^{32}S(^{3}He,α)^{31}S study by Bhatia *et al.* [12]. Examination of Fig. 1 of Ref. [12]

reveals, however, that the observation of this state is tentative. Furthermore, there are no candidate analog levels in ^{31}P or additional states predicted by shell-model calculations in this energy region. We, therefore, conclude that this level likely does not exist.

States in the excitation energy region between 4.9 MeV and the proton-emission threshold, at 6130.9(4) keV [2], are populated in the (^{3}He,t) reaction. See Fig. 3(c) of Ref. [13]. Of these levels only two have previously reported γ-decay information from which angular distributions could be extracted [6,7]. These are the 5302- and 5977-keV states which are both assigned spin-parities of $9/2^+$ in the work of Jenkins *et al.* [6,7]. In the present work, utilizing new γ-decay information, spin-parities are suggested for all states in this energy region, with the states then paired to their ^{31}P

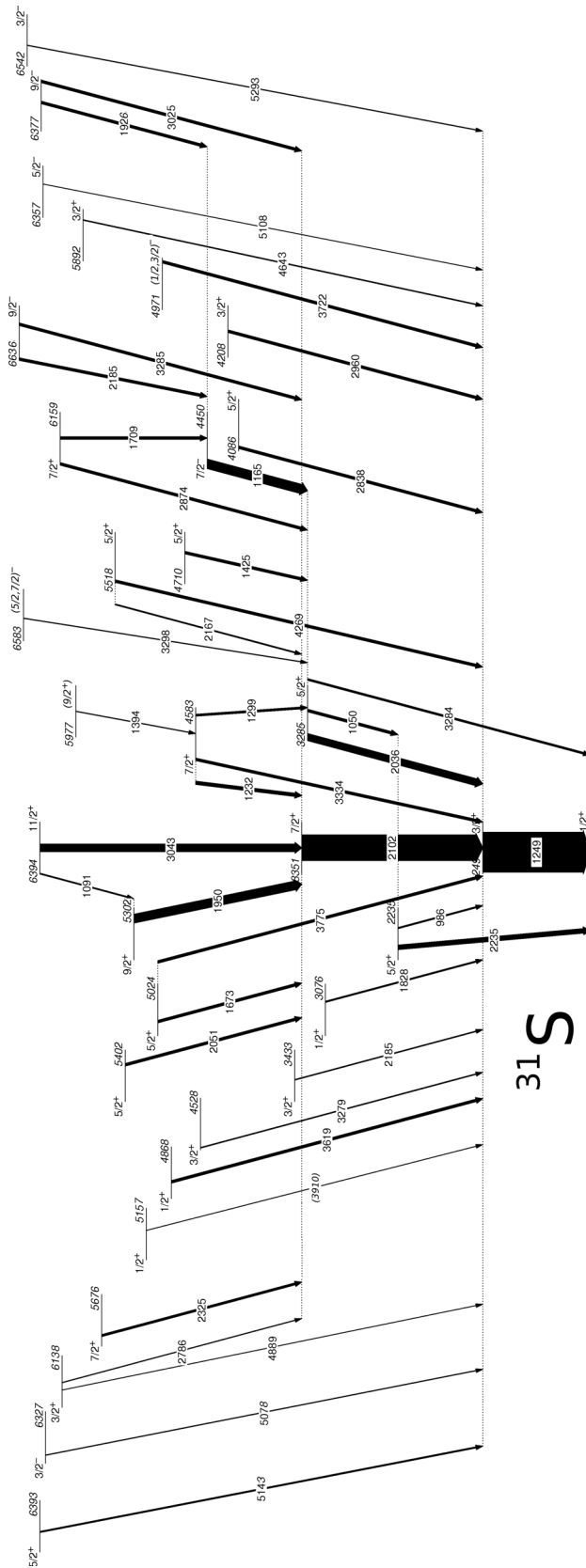FIG. 6. Full γ decay scheme for the nucleus ^{31}S observed in this work. The γ-ray energies are given in keV, while the widths of the arrows represent the measured intensity of the transitions.

analog levels. De-excitations from the 5439-keV state and the neighboring levels at 5775 and 5824 keV are, however, not observed here despite being clearly populated in the ^{31}P(^{3}He, t)^{31}S reaction [13]. The only known unpaired analog state in ^{31}P is the 5559-keV level, see Fig. 8. The 5559-keV level has been previously shown to exhibit a dominant decay branch toward the ground state [11], which this experiment is not sensitive to. The nonobservation of decays from the 5559-keV level, therefore, support this mirror assignment. For the 5775-keV level, the only previously reported γ-decay information is the 3540(3)-keV transition to the $5/2_1^+$, 2235-keV state. Transitions that feed this level cannot be observed in the present work due to the presence of the near degenerate, 2234-keV transition in ^{31}P which is produced much more strongly from the one-proton evaporation channel. The 5824-keV level likely displays similar γ-decay behavior, accounting for its nonobservation in this work.

A. States lying close to the proton-emission threshold for the ^{30}P(p,γ)^{31}S reaction

The 5892-keV state in ^{31}S has been identified previously in transfer reactions where it was assigned a spin-parity of $(3/2,5/2)^+$ [11]. Here we observe its γ decay for the first time as it de-excites via the 4643-keV γ ray towards the $3/2_1^+$ level. The angular distribution obtained for the 4643-keV γ ray suggests a clear $\Delta J = 0$ transition which implies a $3/2^+$ spin-parity assignment for the 5892-keV level, in agreement with the previous assignment [11]. As no other candidate $3/2^+$ levels in this excitation energy region in ^{31}P display only this decay branch, it is assigned as the analogue of the 6158-keV state. This is in contrast to the most recent ^{32}S(d, t) transfer reaction study by Irvine *et al.* [15], where the 6158-keV level is suggested as the analog of the first proton-unbound, ^{31}S state at 6138 keV, see Fig. 3 in Ref. [15]. By examining Fig. 8, it is clear that the 6158-keV state is the only viable candidate mirror level for the 5892-keV state as no other $J = 3/2$ states are observed in ^{31}P or predicted by shell-model calculations. Furthermore, the 6138-keV state is observed to exhibit a decay branch toward the $7/2_1^+$ level, see Table I. Such a branch has also been observed for the 6233-keV ^{31}P level [11] supporting the mirror assignment presented in Fig. 8 and in the work published previously on this data set [5].

In this previous publication [5], the 6160-keV level in ^{31}S was assigned as the mirror partner of the 6399-keV ^{31}P state, based on the decay branches to the $7/2_1^-$ and $5/2_1^+$ levels displayed by both states. However, in the recent work of Irvine *et al.* [15] the 6399-keV ^{31}P level is suggested to be the mirror partner of a new ^{31}S state at an excitation energy of 6402(2) keV. This state is not observed in the present work nor the previous γ-ray spectroscopy study of Jenkins *et al.* [6,7]. Nevertheless, if it does exist and is shown to be the analog of the 6399-keV level in ^{31}P, then a likely alternative ^{31}P analog for the 6160-keV state would be the $7/2^+$, 6046-keV level, which, at present, is not paired with any state in ^{31}S. However, we note that such an assignment would imply a negative mirror energy difference (MED) of $\sim$100 keV, a value not observed for other states in this work or in other studies of
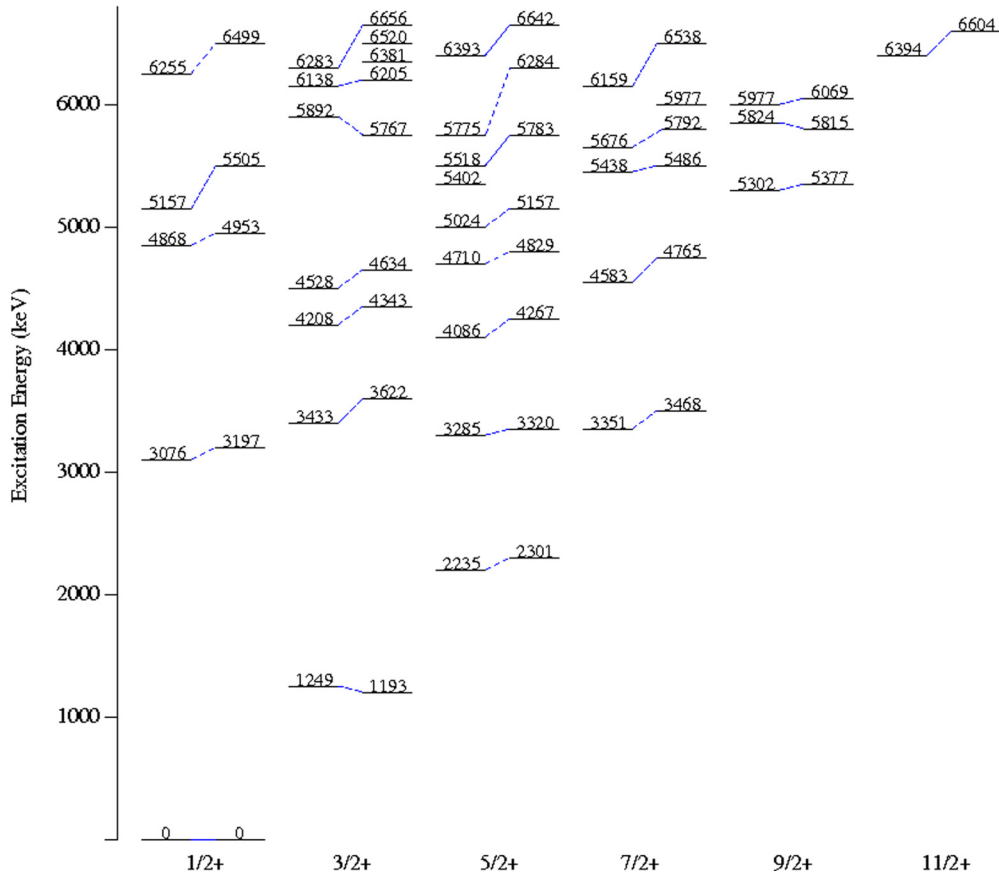
FIG. 7. (Color online) Even-parity excited states in ^{31}S (left) plotted together with a comparison to shell-model calculations (right). For the 6138-keV level with a spin-parity $(3/2,7/2)^+$ a $3/2^+$ assignment is chosen for the purposes of comparison. The $3/2_7^+$, $3/2_8^+$, and $7/2_5^+$ states predicted by the shell model are also shown in the figure but, at present, are not paired with experimentally observed ^{31}S levels.

sd-shell mirror nuclei, e.g., Refs. [1,16,18]. Consequently, the mirror-assignments presented in our previous work [5] are still favored. In the discussion above the differences between the mirror assignments made by Irvine *et al.* [15] and those published in Ref. [5] were highlighted. However, it is important to note that the agreement is in general satisfactory; see Fig. 2 of Ref. [5] and Fig. 3 of Ref. [15], for example.

IV. MIRROR ENERGY DIFFERENCES

The MED values observed in this work are plotted as a function of ^{31}S excitation energy, for both even- and odd-parity states, in Fig. 9; with the MED defined here as $E_x(^{31}$P)-$E_x(^{31}$S). Clearly, a general trend of increasing MEDs with increasing excitation energy is observed, as seen in other sd-shell nuclei; e.g., Ref. [1]. However, no obvious trend between the observed MEDs and the angular momentum of the levels is observed.

The largest shifts, of the order 250 keV, were observed for odd-parity states, as was the case in the $T = 1/2$, $A = 35$ mirror system [16]. Such states are associated with particular configurations where a single nucleon (proton or neutron) is promoted from the sd to the fp shell. In these cases, single-particle effects are critical and lead to larger observed MED values [16].

V. COMPARISON WITH SHELL MODEL CALCULATIONS

Shell-model calculations for the present work were carried out using the universal sd-shell Hamiltonian ($usdpn$) [19]. It is clear, from Figs. 7 and 10 that there is good agreement between even-parity states observed in the present study and shell-model calculations. It can be seen from Fig. 10 that the agreement between the experiment and calculations is typically better than 250 keV. This difference, however, increases with increasing excitation energy. All low-spin and even-parity states can be constructed by considering excitations within the sd-shell only. Such agreement, therefore, provides confidence in using calculations when experimental data are not available, particularly for states at low excitation energy.

Examination of Fig. 7. also reveals a general trend where the experimentally determined even-parity states are located at lower excitation energy than their shell-model counterparts. The largest shifts are observed for levels lying above the proton-emission threshold at 6130.9(4) keV [2]. Extra caution must, therefore, be taken when carrying out comparisons between experimental data and the results of calculations in this energy range. Only four states in this entire energy region exhibit a deviation from this trend with the experiment lying at higher excitation energy than the corresponding shell-model result. Of these states, the largest deviation observed is for the 5892-keV, $3/2_5^+$ level whose shift of +125 keV relative to the
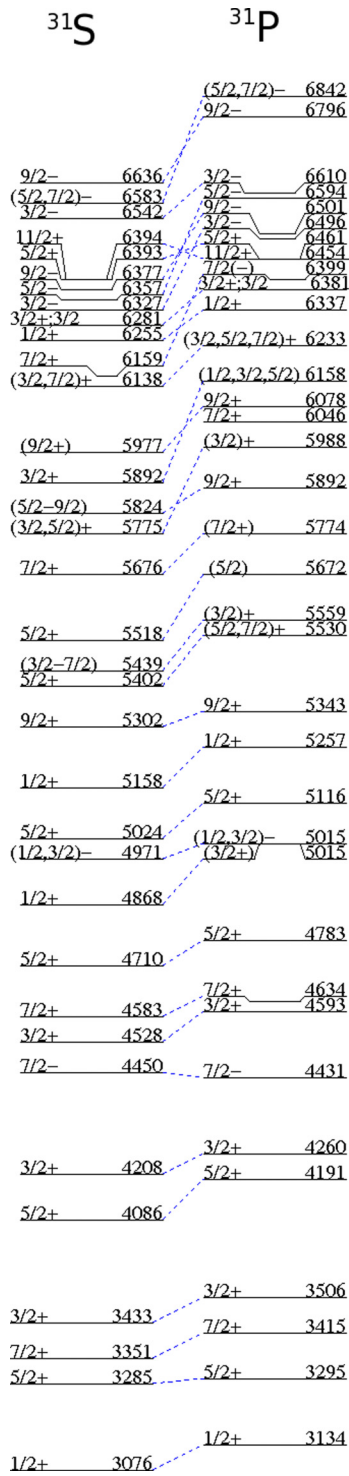
FIG. 8. (Color online) Favored mirror assignments of excited states in ^{31}S (left) for excitation energies between 3 and 6.7 MeV. ^{31}P excitation energies and spin-parity assignments are from the 2013 Nuclear Data Evaluation [11].

shell-model prediction is relatively small when compared with the magnitude of other shifts determined in this work.

To account for odd-parity and higher-spin states, however, it is necessary to introduce intruder configurations involving
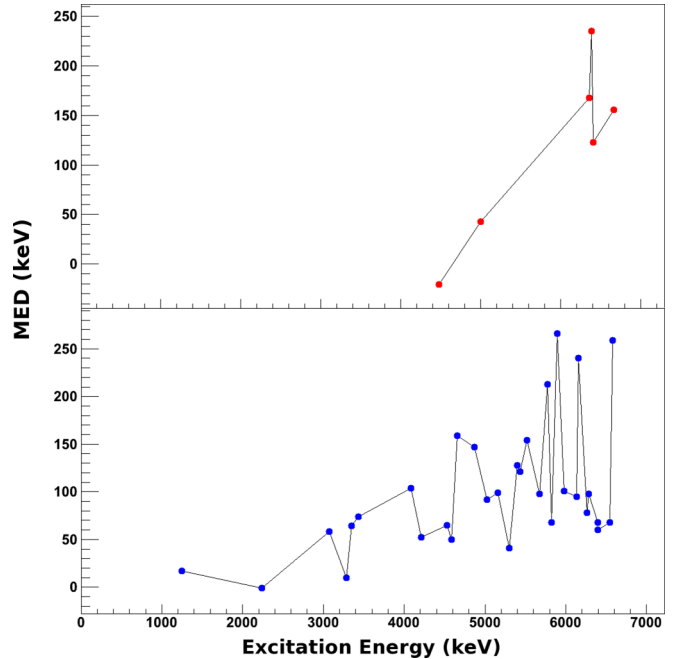

FIG. 9. (Color online) (a) Mirror energy differences observed between odd-parity states in the $T = 1/2$ mirror pair ^{31}S and ^{31}P in the energy region 0–6.7 MeV. (b) Mirror energy differences observed between even-parity states in the $T = 1/2$ mirror pair ^{31}S and ^{31}P in the energy region 0–6.7 MeV.

higher-lying single-particle states. Such shell-model calculations therefore need to include effective interactions between the two main shells, sd and fp. Calculations which include odd-parity states would be particularly interesting for this nucleus as proton-unbound, odd-parity states may correspond to $l_p = 1$ resonances in the ^{30}P $+ p$ system. These resonances can have strong proton spectroscopic factors and, hence could dominate the ^{30}P$(p,\gamma)^{31}$S reaction rate over the temperature range of relevance in ONe novae outbursts.

The shell-model calculations performed by Brown [19] also include predictions of the expected γ-decay branches for the levels. This information proved valuable in the present study to assist with pairing up experimentally observed states
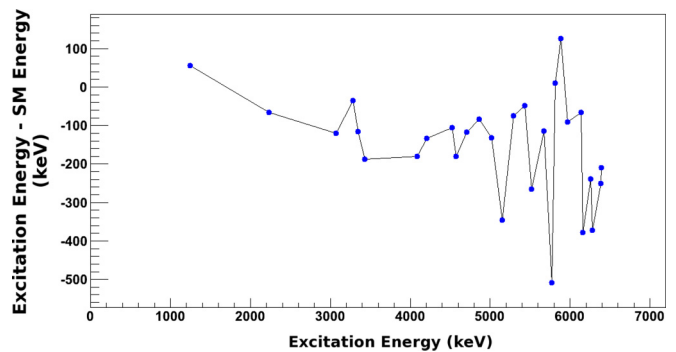

FIG. 10. (Color online) Plot of difference between experimentally determined ^{31}S excitation energies and energies predicted by shell-model calculations.

with the results of calculations. An interesting example is for the doublet of levels observed at an excitation energy of around 6393 keV. An $11/2^+$ state was identified in the previous γ-ray spectroscopy study by Jenkins *et al.* [6,7], however, in our recent work [5], a near degenerate $5/2^+$ state was also observed. The two levels have not previously been distinguished in transfer [20] and charge-exchange reactions [13,14,21] due to their near energy degeneracy. In Ref. [5] the two levels were distinguished by their different decay branches. The $11/2^+$ state exhibits decays to the $7/2_1^+$ and $9/2_1^+$ levels whereas the $5/2^+$ state decays towards the $3/2_1^+$ level. This observation is supported by shell-model calculations [19] which predict a $5/2^+$ at 6642 keV very close in energy to the calculated $11/2_1^+$ state. Furthermore, the decay branches predicted for these levels are in agreement with those observed in the present work. Indeed, all even-parity states above the proton-threshold, which play a role in the ^{30}P$(p,\gamma)^{31}$S capture reaction in novae, have now been paired with the results of shell-model calculations.

VI. CONCLUSIONS

Mirror assignments have been proposed for all states in ^{31}S from the ground state up to an excitation energy of 6.7 MeV, the largest energy of relevance for the ^{30}P$(p,\gamma)^{31}$S reaction in ONe novae environments. In making these assignments, γ rays from a large number of low-spin, excited states have been observed for the first time. This work, therefore, builds on other recent γ-ray spectroscopy studies of light-mass nuclei, relevant to nuclear astrophysics, where the complete level structure is known from the ground state up to the energies of interest in explosive astrophysical scenarios. See for example Refs. [1,10,18].

MEDs between these states have been found to follow a general pattern of increasing with excitation energy. For odd-parity states, however, where single-particle effects are important, large isolated MED values have been observed reinforcing the need for spectroscopic information to propose direct analog assignments. For even-parity states, the agreement between experimental data and shell-model calculations is excellent. Such agreement provides confidence in using calculations in situations where experimental data are absent. However, we also note there are levels predicted by shell model calculations which, at present, have no experimental counterpart.

In addition, future direct measurements of the astrophysical ^{30}P$(p,\gamma)^{31}$S reaction will depend on the experimental spectroscopic information acquired for this $T = 1/2$, $A = 31$ mirror system. Such a direct measurement will require the precise location of excited states in ^{31}S that are thought to be strong resonances in the ^{30}P $+ p$ system. Furthermore, the pairing of excited states in ^{31}S with their ^{31}P counterparts is vital for extracting proton spectroscopic factors from the ^{30}P$(d,p)^{31}$P reaction when radioactive ^{30}P beams of sufficient intensity become available.

[1] G. Lotay, P. J. Woods, D. Seweryniak, M. P. Carpenter, H. M. David, R. V. F. Janssens, and S. Zhu, Phys. Rev. C **84**, 035802 (2011).

[2] A. Kankainen *et al.*, Phys. Rev. C **82**, 052501(R) (2010).

[3] C. Iliadis *et al.*, Astrophys. J. Suppl. **142**, 105 (2002).

[4] J. José, M. Hernanz, and C. Illiadis, Nucl. Phys. A **777**, 550 (2006).

[5] D. T. Doherty, G. Lotay, P. J. Woods, D. Seweryniak, M. P. Carpenter, C. J. Chiara, H. M. David, R. V. F. Janssens, L. Trache, and S. Zhu, Phys. Rev. Lett. **108**, 262502 (2012).

[6] D. G. Jenkins *et al.*, Phys. Rev. C **72**, 031303(R) (2005).

[7] D. G. Jenkins *et al.*, Phys. Rev. C **73**, 065802 (2006).

[8] R. V. F. Janssens and F. S. Stephens, Nucl. Phys. News **6**, 9 (1996).

[9] D. C. Radford, http://radware.phy.ornl.gov

[10] D. Seweryniak, P. J. Woods, M. P. Carpenter, T. Davinson, R. V. F. Janssens, D. G. Jenkins, T. Lauritsen, C. J. Lister, J. Shergur, S. Sinha, and A. Woehr, Phys. Rev. C **75**, 062801(R) (2007).

[11] C. Ouellet and B. Singh, Nucl. Data Sheets **114**, 209 (2013).

[12] T. S. Bhatia, W. W. Daehnick, and G. J. Wagner, Phys. Rev. C **5**, 111 (1972).

[13] C. Wrede, J. A. Caggiano, J. A. Clark, C. M. Deibel, A. Parikh, and P. D. Parker, Phys. Rev. C **79**, 045803 (2009).

[14] C. Wrede, J. A. Caggiano, J. A. Clark, C. M. Deibel, A. Parikh, and P. D. Parker, Phys. Rev. C **76**, 052802(R) (2007).

[15] D. Irvine *et al.*, Phys. Rev. C **88**, 055803 (2013).

[16] J. Ekman *et al.*, Phys. Rev. Lett. **92**, 132502 (2004).

[17] A. Saastamoinen, Ph.D. thesis, University of Jyväskylä, 2011, http://www.jyu.fi/static/fysiikka/vaitoskirjat/2011/Saastamoinen -Antti.pdf

[18] D. G. Jenkins *et al.*, Phys. Rev. C **87**, 064301 (2013).

[19] B. A. Brown, 2013 (private communication).

[20] Z. Ma *et al.*, Phys. Rev. C **76**, 015803 (2007).

[21] A. Parikh *et al.*, Phys. Rev. C **83**, 045806 (2011).